

## Stabilization of vector solitons in optical lattices

Yaroslav V. Kartashov,<sup>1,2</sup> Anna S. Zelenina,<sup>2</sup> Victor A. Vysloukh,<sup>3</sup> and Lluís Torner<sup>1</sup>

<sup>1</sup>*ICFO, Institut de Ciències Fòniques, and Department of Signal Theory and Communications, Universitat Politècnica de Catalunya, 08034 Barcelona, Spain*

<sup>2</sup>*Physics Department, M. V. Lomonosov Moscow State University, 119899, Vorobiovy Gory, Moscow, Russia*

<sup>3</sup>*Departamento de Física y Matemáticas, Universidad de las Américas, Puebla, Santa Catarina Martir, Código Postal 72820, Puebla, Cholula, Mexico*

(Received 16 July 2004; published 27 December 2004)

We address the properties and dynamical stability of one-dimensional vector lattice solitons in a Kerr-type cubic medium with harmonic transverse modulation of the refractive index. We discovered that unstable families of scalar lattice solitons can be stabilized via cross-phase modulation (XPM) in the vector case. It was found that multihumped vector solitons that are unstable in uniform media where the XPM strength is higher than that of self-phase modulation can also be stabilized by the lattice.

DOI: 10.1103/PhysRevE.70.066623

PACS number(s): 42.65.Tg, 42.65.Jx, 42.65.Wi

### I. INTRODUCTION

Light propagation in media whose properties vary periodically in the transverse direction exhibits a wealth of practically interesting phenomena including the formation of stable localized structures, which find applications in many branches of modern physics, including waves in molecular chains [1], trapped Bose-Einstein condensates [2], or solids [3]. In nonlinear optics discrete solitons have been extensively studied and observed in periodic arrays of weakly coupled waveguides [4]. Such strongly localized modes might be used to test all-optical switching and routing concepts. Recently it was shown that lattices constituted by continuous nonlinear media with an imprinted harmonic modulation of the refractive index offer a number of additional opportunities for the manipulation of light signals [5]. Scalar solitons in the harmonic lattices were observed in photorefractive crystals [6] and analyzed in Refs [7,8].

However, the interaction between several light waves can considerably enrich the dynamics of their propagation and open additional perspectives for cross stabilization and all-optical soliton phenomena. In uniform media, two-component bright vector solitons were studied for coherent [9] and incoherent [10] interactions. Strongly localized vectorial *discrete modes* in arrays of evanescently coupled waveguides and their stability were reported in Ref. [11]. Very recently coupling between mutually incoherent solitons belonging to the different bands of the transmission spectrum of periodic lattices was discussed [12], while vector solitons were observed in  $\text{Al}_x\text{Ga}_{1-x}\text{As}$  nonlinear waveguide arrays [13]. However, the investigation of the properties and stability of *vector solitons in optical lattices*, which can be qualitatively and quantitatively altered by variation of the properties of the lattice, is an open problem.

In this work we perform a detailed analysis of the properties and dynamical stability of one-dimensional vector lattice solitons in both focusing and defocusing cubic media. We reveal that cross-phase modulation (XPM) results in stabilization of even (in focusing media) and twisted (in defocusing media) soliton components that are known to be highly unstable in the scalar case. We show that, in contrast

to solitons in uniform media, vector lattice solitons can be made stable if the XPM strength exceeds that of self-phase modulation. We also reveal the existence of stable multihumped vector complexes in which one component is stabilized by the lattice, while the other one is stabilized by XPM.

### II. MODEL

We address the propagation of coupled laser beams along the  $\xi$  axis in media with a periodic modulation of the linear refractive index in the  $\eta$  direction, described by the system of coupled nonlinear Schrödinger equations

$$i \frac{\partial q_1}{\partial \xi} = -\frac{1}{2} \frac{\partial^2 q_1}{\partial \eta^2} + \sigma q_1 (|q_1|^2 + C|q_2|^2) - pR(\eta)q_1,$$

$$i \frac{\partial q_2}{\partial \xi} = -\frac{1}{2} \frac{\partial^2 q_2}{\partial \eta^2} + \sigma q_2 (C|q_1|^2 + |q_2|^2) - pR(\eta)q_2, \quad (1)$$

where  $\eta$  and  $\xi$  are scaled to the beam width and diffraction length, respectively;  $C$  is the XPM parameter;  $\sigma = \mp 1$  for the focusing and defocusing media;  $p$  is the guiding parameter; the function  $R(\eta) = \cos(2\pi\eta/T)$  describes the refractive index profile; and  $T$  is the lattice period. The XPM coefficient in Eqs. (1) depends on the particular settings and materials involved. Thus for mutually incoherent light beams  $C=1$  [10,14], while for coherent orthogonally polarized beams interacting in highly birefringent media  $C=2$  [9,15]. The parameter  $C$  can acquire quite high values in organic materials [9]. Notice also that photorefractive crystals offer additional possibilities for manipulation of the XPM coupling, by varying the polarization of the light beams or the elements of the electro-optic tensor involved [6]. Equations (1) admit several conserved quantities including the total  $U$  and partial  $U_{1,2}$  energy flows:

$$U = U_1 + U_2 = \int_{-\infty}^{\infty} (|q_1|^2 + |q_2|^2) d\eta. \quad (2)$$

### III. VECTOR SOLITON FAMILIES

Stationary solutions of Eqs. (1) have the form  $q_{1,2}(\xi, \eta) = w_{1,2}(\eta)\exp(ib_{1,2}\xi)$ , where  $w_{1,2}(\eta)$  are real functions and  $b_{1,2}$  are real propagation constants. Lattice soliton families are defined by  $b_{1,2}$ , the lattice period  $T$ , and the parameters  $p$  and  $C$ . Since one can use the scaling transformation  $q_{1,2}(\eta, \xi, p, C) \rightarrow \chi q_{1,2}(\chi\eta, \chi^2\xi, \chi^2p, C)$  to obtain various families of solutions from a given one, the transverse scale was selected in such a way that the modulation period  $T = \pi/2$  is a constant, and  $b_{1,2}$ ,  $p$ , and  $C$  are variable parameters. Upon linear stability analysis we searched for perturbed solutions of Eqs. (1) in the form  $q_{1,2}(\eta, \xi) = [w_{1,2}(\eta) + u_{1,2}(\eta, \xi) + iv_{1,2}(\eta, \xi)]\exp(ib_{1,2}\xi)$ , where the real  $u_{1,2}$  and imaginary  $v_{1,2}$  parts of the small perturbation can grow with a complex growth rate  $\delta$ . The standard linearization procedure around the stationary solution  $w_{1,2}$  for Eqs. (1) yields the linear eigenvalue problem

$$\begin{aligned} \delta u_1 &= -\frac{1}{2} \frac{d^2 v_1}{d\eta^2} + [\sigma(w_1^2 + Cw_2^2) + b_1]v_1 - pRv_1, \\ \delta v_1 &= \frac{1}{2} \frac{d^2 u_1}{d\eta^2} - [\sigma(3w_1^2 + Cw_2^2) + b_1]u_1 - 2\sigma Cw_1w_2u_2 + pRu_1, \\ \delta u_2 &= -\frac{1}{2} \frac{d^2 v_2}{d\eta^2} + [\sigma(w_2^2 + Cw_1^2) + b_2]v_2 - pRv_2, \\ \delta v_2 &= \frac{1}{2} \frac{d^2 u_2}{d\eta^2} - [\sigma(3w_2^2 + Cw_1^2) + b_2]u_2 - 2\sigma Cw_1w_2u_1 + pRu_2 \end{aligned} \quad (3)$$

for the perturbation components  $u_{1,2}, v_{1,2}$ , which was solved numerically. The scaling transformation mentioned above predicts changes of the growth rate for unstable solitons with identical functional profiles supported by lattices with different periods. For example, if the lattice period becomes  $\chi$  times smaller then the corresponding growth rate increases  $\chi^2$  times.

We start our analysis by recalling the properties of *scalar* lattice solitons. There exist odd, even, and twisted scalar lattice solitons. In focusing media odd solitons are stable, even ones are unstable, and twisted ones are stable above a certain energy threshold. Defocusing media support stable odd and even solitons, but twisted solitons are unstable. The simplest vector soliton solutions are formed at  $b_1 = b_2$ , when  $w_1(\eta) = w(\eta)\cos\phi$ ,  $w_2(\eta) = w(\eta)\sin\phi$ , where  $w(\eta)$  is the scalar soliton profile, and  $\phi$  is a phase. The most interesting situation occurs at  $b_1 \leq b_2$ , when the first and second components have different types of symmetry. Below we focus on the simplest self-sustained structures, having a twisted first component  $w_1$ . Such vector solitons can be classified according to the field distribution in the second component.

#### A. Odd solitons in focusing media

The properties of *odd* vector solitons in focusing media are summarized in Fig. 1 at  $C=1$ . At low energy flows the

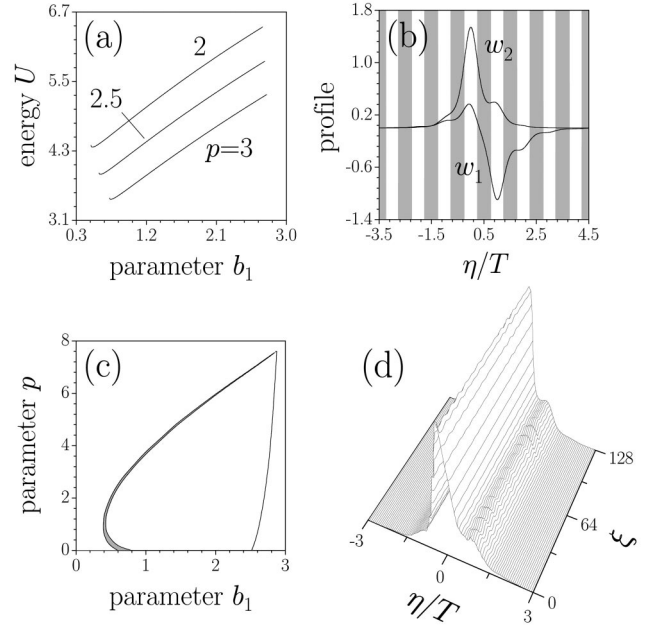


FIG. 1. (a) Energy flow of odd soliton versus propagation constant  $b_1$  at  $b_2=3$  and various guiding parameters. (b) Profile of odd soliton at  $b_1=0.7, b_2=1.5, p=2$ . (c) Areas of stability and instability (shaded) for odd solitons on  $(b_1, p)$  plane at  $b_2=3$ . (d) Stable propagation of odd soliton depicted in (b) in the presence of white noise with variance  $\sigma_{1,2}^2=0.01$ . In (d) only the second component is shown. Focusing medium  $\sigma=-1, C=1$ . All quantities are plotted in arbitrary dimensionless units.

second component of the odd soliton has a single well-defined maximum coinciding with the local maximum of  $R(\eta)$ , so that the field distribution in both second and first components is asymmetric [Fig. 1(b)]. There exist lower and upper cutoffs on  $b_1$  at fixed  $b_2$  and  $p$  [Fig. 1(a)]. As  $b_1$  approaches the upper cutoff, the second component develops two equal humps located on neighboring lattice sites; this means that the odd vector soliton transforms into the even one. At the lower cutoff the odd soliton ceases to exist. Energy flow versus  $b_1$  is shown in Fig. 1(a) at fixed  $b_2$  and  $p$ . The energy flow drops off with growth of the guiding parameter at fixed  $b_1$  and  $b_2$ . At  $U, U_{1,2} \rightarrow \infty$ , the odd vector soliton transforms into weakly coupled scalar and vector solitons located at neighboring sites. The area of existence of the odd soliton first expands and then shrinks with growth of the guiding parameter  $p$  [Fig. 1(c)] for fixed  $b_2$ , so odd solitons cease to exist when the guiding parameter  $p$  exceeds the critical value. The width of the existence area increases with growth of  $b_2$ . Notice that there is lower threshold on  $b_2$  for the existence of odd solitons.

#### B. Even solitons in focusing media

The properties of *even* vector solitons (composed of the twisted first and even second components) are summarized in Fig. 2. The second component has two equal intensity maxima located on neighboring sites [Fig. 2(b)]. The total energy flow decreases monotonically with growth of  $b_1$  at

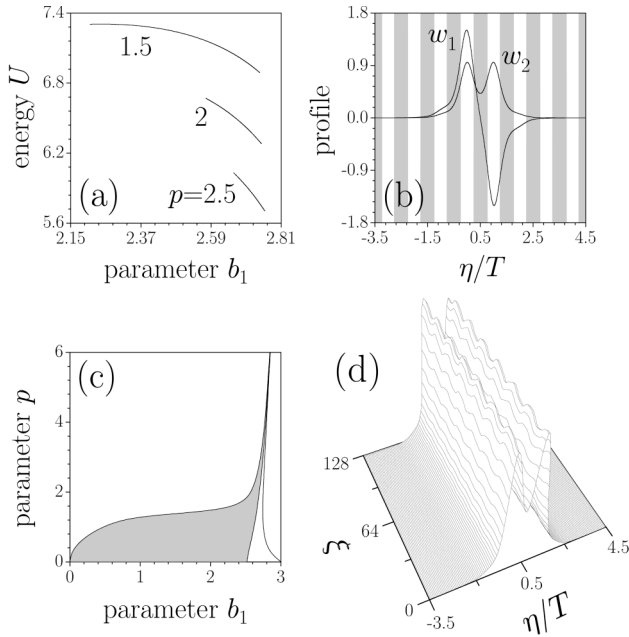


FIG. 2. (a) Energy flow of even soliton versus propagation constant  $b_1$  at  $b_2=3$  and various guiding parameters. (b) Profile of even soliton at  $b_1=1.65, b_2=2, p=2$ . (c) Areas of stability and instability (shaded) for even solitons on  $(b_1, p)$  plane at  $b_2=3$ . (d) Stable propagation of even soliton depicted in (b) in the presence of white noise with variance  $\sigma_{1,2}^2=0.01$ . In (d) only the second component is shown. Focusing medium  $\sigma=-1, C=1$ . All quantities are plotted in arbitrary dimensionless units.

fixed  $b_2, p$ , and drops off with increase of  $p$  at fixed  $b_1, b_2$  [Fig. 2(a)]. There are lower and upper cutoffs on  $b_1$ . At the lower cutoff  $w_1 \rightarrow 0$ , and the vector soliton transforms into an even scalar soliton, while at the upper cutoff  $w_2 \rightarrow 0$ , and it converts into a twisted scalar soliton. The existence area of the even soliton expands with decrease of the guiding parameter  $p$  and slightly changes with growth of  $b_2$  [Fig. 2(c)].

### C. Soliton stability in focusing media

The results of the stability analysis are summarized in Figs. 1 and 2. We have found that *odd* vector solitons are stable almost in the whole domain of their existence [Fig. 1(c)], a result confirmed by numerical integration of Eqs. (1) in the presence of input noise [Fig. 1(d)]. The linear stability analysis also revealed the existence of stability bands for *even* vector solitons. They turn out to be stable when the amplitude of the first twisted component becomes large enough. Therefore XPM can stabilize the otherwise unstable soliton component. This is one of the most important results of this work.

Soliton stabilization occurs because of local increase of the refractive index in neighboring lattice sites created by stable twisted component via XPM. This local increase prevents the even component from decaying into the odd one under the action of perturbations. The onset of stability is dictated by the peak amplitude or energy  $U_1$  of the twisted component, the ratio  $U_1/U_2$ , and the depth of the optical

lattice that can be flexibly controlled in distinction from discrete systems. Since the lower amplitudes are necessary to support solitonlike propagation in deeper lattices, stabilizing action of the twisted component and the width of the stability domain decrease with growth of  $p$ . Notice that the upper boundary of the instability domain for the even vector soliton coincides with the upper cutoff for the odd one, i.e., the latter transforms into the stable even soliton at the upper cutoff. Figure 2(d) illustrates the stable propagation of the even lattice soliton perturbed by noise.

### D. Odd and even solitons in defocusing media

Optical lattices in defocusing media also support vector solitons, but those are typically wider than their counterparts in focusing media. The energy flow of the *even* soliton versus  $b_1$  is depicted in Fig. 3(a), while Fig. 3(b) shows the profile of such a soliton. The energy flow increases with growth of  $p$  at fixed  $b_1, b_2$ . Notice that in defocusing media at the upper cutoff on  $b_1$  the first component vanishes and the vector soliton transforms into the even scalar one, while at the lower cutoff on  $b_1$  the second component vanishes and one gets a twisted scalar soliton. The area of existence for even solitons on the  $(b_1, p)$  plane broadens with decrease of the guiding parameter [Fig. 3(c)] at fixed  $b_2$ . The width of the existence area on  $b_1$  decreases linearly with growth of the propagation constant  $b_2$  at fixed  $p$ , so that above a certain threshold on  $b_2$  even solitons cease to exist. We have also found *odd* vector solitons in a defocusing medium [Fig. 3(e)]. Its first component transforms into a linear Bloch wave at the lower cutoff on  $b_1$ , while the second one remains localized. The odd soliton converts into the stable even soliton at the upper cutoff on  $b_1$ .

### E. Soliton stability in defocusing media

Results of the stability analysis are summarized in Fig. 3(c). We discovered the existence of a stability band for even vector solitons. Thus in defocusing optical media the twisted first component (which is unstable alone) can be stabilized through XPM interaction with the stable even second component. Cross stabilization takes place if the amplitude of the second even component is large enough, actually near the upper cutoff for existence. The stability area for even vector solitons shrinks at low  $p$ . Figure 3(d) shows stable propagation of the even soliton in defocusing media in the presence of white input noise. The stability analysis for odd solitons becomes complicated near the lower cutoff (area of weak localization) but we have found that they are stable near the upper edge of the existence domain on  $b_1$  [Fig. 3(f)]. The important result is that the combined action of the lattice and XPM enables stabilization of vector solitons of *high order*, to be perhaps referred to as *vector soliton trains*, with a complex multihumped intensity profile, when one of the component's is a scalar soliton train.

### F. Impact of XPM strength on soliton stability

We also analyzed the impact of XPM strength on the stability of vector lattice solitons. The most important result is

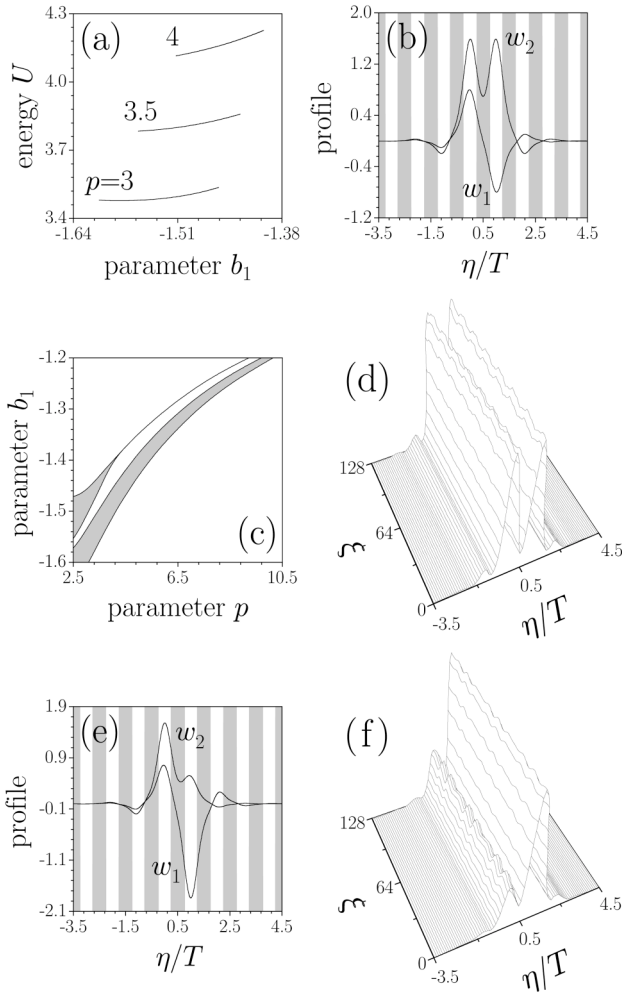


FIG. 3. (a) Energy flow of even soliton versus propagation constant  $b_1$  at  $b_2=-1$  and various guiding parameters. (b) Profile of even soliton at  $b_1=-1.36, b_2=-1, p=5$ . (c) Areas of stability and instability (shaded) for even solitons on  $(b_1, p)$  plane at  $b_2=-1$ . (d) Stable propagation of even soliton depicted in (b) in the presence of white noise with variance  $\sigma_{1,2}^2=0.01$ . (e) Profile of odd soliton at  $b_1=-1.6, b_2=-1, p=5$ . (f) Stable propagation of odd soliton depicted in (e) in the presence of white noise with variance  $\sigma_{1,2}^2=0.01$ . In (d) and (f) only the first component is shown. Defocusing medium  $\sigma=1, C=1$ . All quantities are plotted in arbitrary dimensionless units.

that the stability window for bright even lattice solitons exists at  $C \neq 1$  [Fig. 4(a)] in contrast to the case of uniform media, where multihumped vector solitons are unstable at  $C > 1$  in the entire domain of their existence, and the width of the stability window can be increased with increase of lattice depth. Notice that the even soliton component vanishes at the lower cutoff on  $b_1$  at  $C \gtrsim 1.03$  thus resulting in stabilization of the vector soliton, while at  $C < 1.03$  the even component vanishes at the upper cutoff [Fig. 4(a)].

Stabilization via XPM is also possible when the first soliton component is subject to the influence of the lattice ( $p \neq 0$ ) while for the second component the medium is uniform ( $p=0$ ). It was revealed that XPM may result in a completely stable twisted-twisted soliton combination [Fig. 4(b)] that

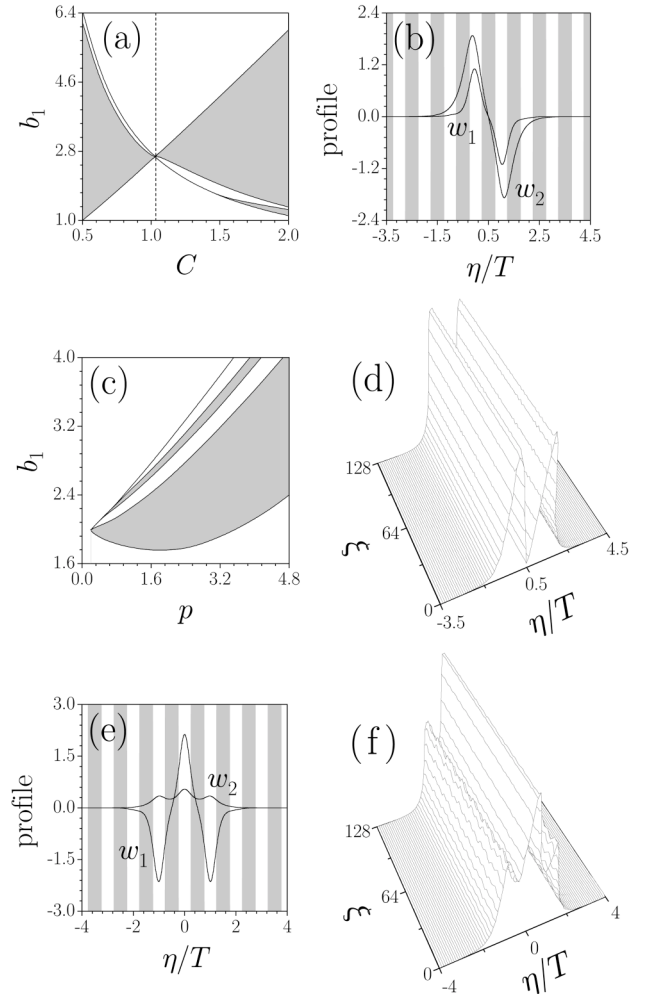


FIG. 4. (a) Areas of stability and instability (shaded) for even solitons on  $(C, b_1)$  plane at  $b_2=3, p=2$ . (b) Profile of twisted soliton in the uniform medium supported by twisted lattice soliton at  $b_1=3.8, b_2=2, p=4$ , and (c) areas of stability and instability (shaded) for such solitons on the  $(b_1, p)$  plane at  $b_2=2$ . (d) Stable propagation of soliton depicted in (b) in the presence of white noise. (e) Profile of three-humped soliton in a uniform medium supported by twisted lattice soliton at  $b_1=3.57, b_2=2, p=4$ , and (f) its stable propagation in the presence of white noise. In (d) and (f) only the second component is shown. Focusing medium  $\sigma=-1$ . All quantities are plotted in arbitrary dimensionless units.

does not exist in a uniform medium. In this case even the weak first “lattice” component can capture and stabilize the strong second “uniform” component. The existence and stability domains broaden with growth of the lattice depth in the first component [Fig. 4(c)]. Because of the alternating sign of the “lattice” component in neighboring sites, the “uniform” component also acquires a multihumped structure [Fig. 4(e)], but still shows stable propagation [Fig. 4(f)].

#### IV. CONCLUSIONS

In conclusion, we analyzed the properties of vector lattice solitons in cubic nonlinear media with harmonic transverse

modulation of the linear refractive index, and discovered that stable propagation sustained by XPM is possible even if one of the soliton components is otherwise unstable. Here we reported only the simplest examples of vector lattice solitons but the results are expected to hold for more general settings and for richer field distributions, including the formation of stable soliton trains. We stress that the combined action of the lattice with tunable strength and XPM offers opportunities not only to alter the *quantitative* characteristics of soli-

tons, but also to control their *qualitative* features, including their topological structure and stability.

#### ACKNOWLEDGMENTS

This work has been partially supported by the Generalitat de Catalunya, by the Spanish Government through Grant No. BFM2002-2861, and by the Russian Foundation for Basic Research through Grant No. 03-02-16370.

- 
- [1] A. S. Davydov and N. I. Kislukha, *Phys. Status Solidi B* **59**, 465 (1973).  
[2] A. Trombettoni and A. Smerzi, *Phys. Rev. Lett.* **86**, 2353 (2001).  
[3] W. P. Su *et al.*, *Phys. Rev. Lett.* **42**, 1698 (1979).  
[4] D. N. Christodoulides and R. I. Joseph, *Opt. Lett.* **13**, 794 (1988); D. N. Christodoulides *et al.*, *Nature (London)* **424**, 817 (2003); H. S. Eisenberg *et al.*, *Phys. Rev. Lett.* **81**, 3383 (1998); R. Morandotti *et al.*, *ibid.* **83**, 2726 (1999).  
[5] Y. V. Kartashov *et al.*, *Opt. Lett.* **29**, 766 (2004); **29**, 1102 (2004); *Opt. Express* **12**, 2831 (2004).  
[6] N. K. Efremidis *et al.*, *Phys. Rev. E* **66**, 046602 (2002); J. W. Fleischer *et al.*, *Phys. Rev. Lett.* **90**, 023902 (2003); *Nature (London)* **422**, 147 (2003); D. Neshev *et al.*, *Opt. Lett.* **28**, 710 (2003).  
[7] N. K. Efremidis *et al.*, *Phys. Rev. Lett.* **91**, 213906 (2003).  
[8] P. J. Y. Louis *et al.*, *Phys. Rev. A* **67**, 013602 (2003); N. K. Efremidis and D. N. Christodoulides, *ibid.* **67**, 063608 (2003).  
[9] V. Manakov, *Sov. Phys. JETP* **38**, 248 (1974); D. N. Christodoulides and R. I. Joseph, *Opt. Lett.* **13**, 53 (1988); J. U. Kang *et al.*, *Phys. Rev. Lett.* **76**, 3699 (1996); N. Akhmediev *et al.*, *ibid.* **81**, 4632 (1998).  
[10] M. Mitchell *et al.*, *Phys. Rev. Lett.* **80**, 4657 (1998); G. I. Stegeman and M. Segev, *Science* **286**, 1518 (1999); E. A. Ostrovskaya *et al.*, *Phys. Rev. Lett.* **83**, 296 (1999); C. Cambournac *et al.*, *ibid.* **89**, 083901 (2002).  
[11] S. Darmanyan *et al.*, *Phys. Rev. E* **57**, 3520 (1998).  
[12] O. Cohen *et al.*, *Phys. Rev. Lett.* **91**, 113901 (2003); A. A. Sukhorukov and Y. S. Kivshar, *ibid.* **91**, 113902 (2003).  
[13] D. Mandelik *et al.*, *Phys. Rev. Lett.* **90**, 253902 (2003); J. Meier *et al.*, *ibid.* **91**, 143907 (2003).  
[14] M. Mitchell *et al.*, *Phys. Rev. Lett.* **79**, 4990 (1997).  
[15] C. R. Menyuk, *IEEE J. Quantum Electron.* **23**, 174 (1987); **25**, 2674 (1989).